

## LETTERS

# Substrate-enhanced supercooling in AuSi eutectic droplets

T. U. Schüll<sup>1,2</sup>, R. Daudin<sup>1</sup>, G. Renaud<sup>1</sup>, A. Vaysset<sup>1</sup>, O. Geaymond<sup>3</sup> & A. Pasturel<sup>4</sup>

The phenomenon of supercooling in metals—that is, the preservation of a disordered, fluid phase in a metastable state well below the melting point<sup>1</sup>—has led to speculation that local atomic structure configurations of dense, symmetric, but non-periodic packing act as the main barrier for crystal nucleation<sup>2,3</sup>. For liquids in contact with solids, crystalline surfaces induce layering of the adjacent atoms in the liquid<sup>4,5</sup> and may prevent or lower supercooling<sup>6</sup>. This seed effect is supposed to depend on the local lateral order adopted in the last atomic layers of the liquid in contact with the crystal. Although it has been suggested that there might be a direct coupling between surface-induced lateral order and supercooling<sup>6</sup>, no experimental observation of such lateral ordering at interfaces is available<sup>6</sup>. Here we report supercooling in gold-silicon (AuSi) eutectic droplets, enhanced by a Au-induced ( $6 \times 6$ ) reconstruction of the Si(111) substrate. *In situ* X-ray scattering and *ab initio* molecular dynamics reveal that pentagonal atomic arrangements of Au atoms at this interface favour a lateral-ordering stabilization process of the liquid phase. This interface-enhanced stabilization of the liquid state shows the importance of the solid–liquid interaction for the structure of the adjacent liquid layers. Such processes are important for present and future technologies, as fluidity and crystallization play a key part in soldering and casting, as well as in processing and controlling chemical reactions for microfluidic devices or during the vapour–liquid–solid growth of semiconductor nanowires.

Clusters with icosahedral short-range order are now widely considered as basic structural elements of liquid metals and glasses<sup>3,7–9</sup>. Their presence has been proven experimentally<sup>4,7,10</sup> and by *ab initio* molecular dynamics simulations (MDS)<sup>11</sup>. At solid–liquid interfaces, however, a description of the structure of liquids is difficult, as is the prediction of the influence of interfaces on ordering and more particularly supercooling. As highlighted in ref. 6, the degree to which a liquid can be supercooled strongly depends on the substrate in contact with it, as well as on thermal history. In recent experiments, enhanced layering in liquids at solid (crystalline)–liquid interfaces has been observed<sup>4,5</sup>. However, tracking its influence on crystallization or supercooling requires an investigation of ordering in the liquid along the interface, which presents an experimental challenge. In the present work, we analyse the influence of different interfaces on the degree of supercooling and possible in-plane order in AuSi liquid droplets of near-eutectic composition. The effects of three substrates—Si(001), Si(111) with a Au-induced ( $\sqrt{3} \times \sqrt{3}$ )R30° reconstruction, and Si(111) with a Au-induced ( $6 \times 6$ ) reconstruction—are compared. Offering fluidity at low temperatures, such eutectic liquids are at the heart of the catalytic growth of semiconductor nanowires by the vapour–liquid–solid process<sup>12</sup>. Recent *in situ* microscopy studies of the growth dynamics and nucleation of semiconductor nanowires<sup>13–15</sup> suggest that Ge nanowires can grow below the AuGe eutectic temperature<sup>16,17</sup>, with the catalysts' state depending

on thermal history. Furthermore, a possible modification of the eutectic temperature for nanostructures has been suggested<sup>18</sup>. These puzzling observations call for further investigations of the supercooling behaviour of metal–semiconductor alloys and their atomic structure at semiconductor interfaces.

We used *in situ* grazing incidence X-ray scattering in ultrahigh vacuum at beamline BM32 of the European Synchrotron Radiation Facility to study solid–liquid transitions on surfaces and nanostructures<sup>4,19</sup>. The experimental results were compared to *ab initio* MDS<sup>11</sup>. The experiment consisted in analysing, for different temperatures, the atomic structure of the silicon surface, that of the liquid/solid Au(Si) islands, and that of the AuSi/Si(111) (or AuSi/Si(001)) interface, special attention being paid to a potential correlation between them. The different steps of the experiment are schematically shown in Fig. 1. The complexity of this system required mapping extended regions in reciprocal space (Fig. 2a), to address all structural features at a given temperature. These extended reciprocal space maps were performed by variation of the momentum transfer  $Q = 4\pi \sin(\theta)/\lambda$ , where  $\lambda$  is the X-ray wavelength and  $\theta$  half the scattering angle between the incident and scattered beams that are almost parallel to the sample surface (for details on experimental tools and sample preparation, see Methods Summary, Supplementary Information, and Supplementary Figs 2 and 4).

During annealing (Fig. 1, steps 2–3), the Au islands transform into liquid droplets exactly at the bulk eutectic temperature,  $T_E = 636 \pm 5$  K, suggesting that the Si substrate provided atoms to reach the Au<sub>81</sub>Si<sub>19</sub> eutectic composition. All diffraction peaks from Au disappear simultaneously at  $T_E$  and give way to a scattering signal that is characteristic of a liquid phase, as shown on the reciprocal space map of Fig. 2a. For annealing temperatures higher than  $T_E + 40$  K (=676 K) and subsequent cooling (Fig. 1, step 4) more diffraction peaks appear, corresponding to a well defined Si(111)-( $6 \times 6$ ) superstructure<sup>20</sup>, as revealed in the reciprocal space map in Fig. 2a. When cooling down below  $T_E$ , no Bragg peaks from solid Au reappear, but the liquid-like scattering remains: the islands stay liquid. Cooling down further reveals that solidification happens only at  $T_S = 513 \pm 5$  K (Fig. 1, step 5), that is, more than 120 K below  $T_E$ . After solidification, the ( $6 \times 6$ ) superstructure remains, together with powder diffraction rings from the face-centred-cubic (f.c.c.) Au structure. Reciprocal space maps for different sample preparations are shown in Supplementary Fig. 4.

Remarkably, this phase transition is found to be fully reproducible: when the temperature is cycled down and up, the above-described behaviour of the solid–liquid–solid transition remains: melting at  $T_E$  on heating, and solidification at  $T_S = 513 \pm 5$  K on cooling. Moreover, the final  $T_S$  value is independent of the time spent (between a few tens of minutes to a few tens of hours) at  $T_S$  or between  $T_S$  and  $T_E$ . Several samples were investigated with the procedure described above, or with co-deposition of an Au<sub>81</sub>Si<sub>19</sub> film with the eutectic composition, all

<sup>1</sup>CEA, Institut Nanosciences et Cryogénie, SP2M, 17 rue des Martyrs, 38054 Grenoble, France. <sup>2</sup>European Synchrotron Radiation Facility, BP 220, 38043 Grenoble, France. <sup>3</sup>Institut Néel, CNRS, BP 166, 38042 Grenoble, France. <sup>4</sup>SIMAP INPG, BP 75, 38402 Saint Martin d'Hères cedex, France.

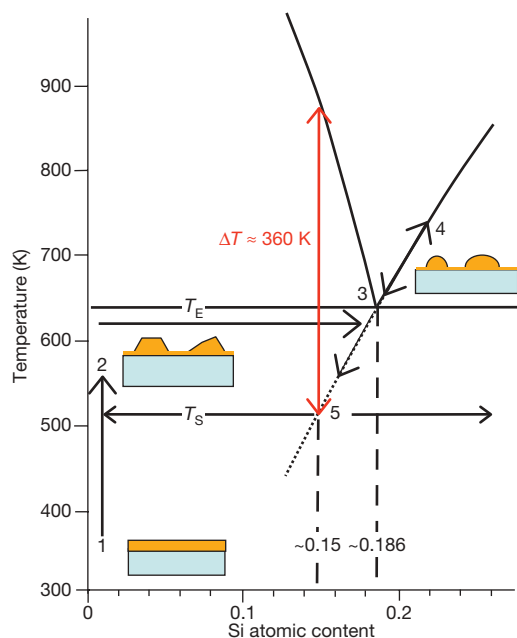


**Figure 1 | Extract from the bulk AuSi phase diagram together with representations of the melting and solidification cycles of AuSi islands on an Si(111)-(6 × 6) reconstructed surface.** The numbers 1 to 5 refer to successive experimental steps, and the large black arrows indicate the pathways followed by the islands during heating/cooling cycles. Seven monolayers of Au are deposited at room temperature (step 1; bottom inset). On annealing they transform into crystalline Au islands (step 2; middle inset). At  $T_E = 636$  K, melting sets in and AuSi droplets with the eutectic composition ( $\text{Au}_{81.4}\text{Si}_{18.6}$ ) are formed (step 3; top right inset). Heating up to 673 K before cooling (step 4) induces a (6 × 6) reconstruction, and leads to a preservation of the liquid phase down to 513 K (step 5), where phase separation and solidification occur (step 5). Above  $T_E$ , on heating or cooling, the liquid composition is expected to follow the Si liquidus. Below  $T_E$ , it follows the (extrapolated; dotted line) metastable Si liquidus. The degree of supercooling (red arrow) has to be measured between this latter and the Au liquidus above  $T_E$  for the corresponding composition of ~15 at.% Si. It amounts to ~360 K.

showing the same solidification temperature after cyclic melting and solidification.

The structure factor  $S(Q)$  of the liquid in its supercooled state is shown in Fig. 3a. Very close to the origin (Fig. 3b), powder diffraction peaks are present, located exactly at the positions expected for the two-dimensional Au-Si crystalline structures reported to form on the surface of the liquid eutectic<sup>21</sup>. Figure 3e shows the intensity evolution around the first maximum of  $S(Q)$  for decreasing temperatures through  $T_S = 513$  K. The initially very broad intensity distribution narrows progressively approaching the solidification temperature, below which it collapses to give rise to the Au(111) Bragg peak. Hysteresis loops extracted from the integrated intensity of Au Bragg reflections (Supplementary Fig. 2) are shown in Fig. 3c for different Si surfaces and/or surface preparation. The lowest solidification temperature  $T_S = 513 \pm 5$  K is observed for droplets on an Si(111)-(6 × 6) surface reconstruction, whereas it is significantly higher ( $T_S = 563 \pm 5$  K) when heating the sample just above  $T_E$ , which only yields a precursory  $(\sqrt{3} \times \sqrt{3})R30^\circ$  reconstruction (Supplementary Fig. 4c). Proceeding similarly on an Si(001) surface (on which no reconstruction coexists with the liquid) only yields  $T_S = 573 \pm 5$  K (Supplementary Fig. 3b). In all cases, peaks of the two-dimensional AuSi surface crystallites (Fig. 3b) were present and the deposited amount of Au was identical, leading to droplet sizes of 150–200 nm, too large to influence the solidification temperature. Remarkably, the size dependence is found to be weak for deposits between two and seven monolayers of Au ( $T_S = (510\text{--}520) \pm 5$  K). One sample with a 30-monolayer Au deposit was investigated, yielding  $T_S = 555 \pm 10$  K (Supplementary Fig. 7). This last value approaches that of  $T_S = 573 \pm 5$  K, obtained when the Si

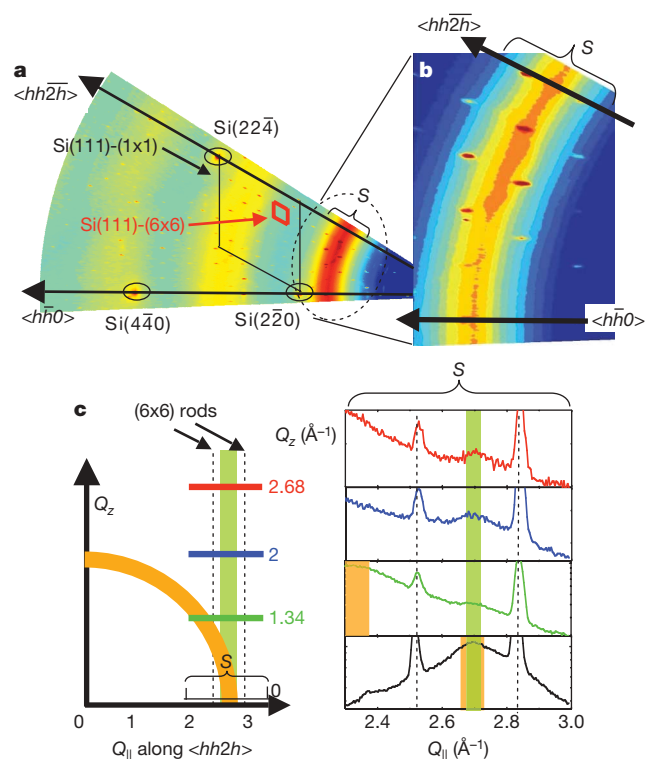


**Figure 2 | Reciprocal space mapping of liquid AuSi islands on (6 × 6) reconstructed Si(111).** **a**, Reciprocal space map of the liquid in its supercooled state on a (6 × 6) reconstructed Si(111) surface. Blue colour corresponds to low intensity, and red to high intensity, yellow being intermediate. Three bulk Bragg peaks are visible, together with a mesh of smaller peaks arising from the (6 × 6) surface/interface periodic superstructure. The three diffuse rings correspond to liquid-like scattering. **b**, Anisotropy of the first order maximum of the liquid structure factor: In the vicinity of strong (6 × 6) reconstruction peaks the signal from the liquid is enhanced, underlining morphological similarities between the crystalline surface and the adjacent liquid layers. **c**, Right: scans across the first order maximum of the liquid structure factor in the plane (along section S marked in **a** and **b**) and parallel to it for several values of out-of-plane momentum transfer,  $Q_z$ . Left: the sketch indicates in orange the position of the first maximum of the isotropic liquid. The green rod corresponds to the intensity distribution stemming from preferential in-plane order.

surfaces suffered from non-ideal preparation conditions (for example, carbon pollution), and is similar to values observed in a closed AuSi system without Si reservoir<sup>22</sup>.

The decrease of the solidification temperature  $T_S$  when the surface is reconstructed (that is, the Si(111)-(6 × 6)Au reconstruction) and with increasing interface/volume ratio shows the crucial role of this particular interface structure on the conservation of the liquid state. This suggests that the specific local atomic structure at the interface favours peculiar ordering effects in the adjacent liquid layers, eventually lowering the interface energy and rendering it a particularly inefficient nucleant for Au. Other crystallization mechanisms may be dominant, such as faceting of the free surface<sup>23</sup> or homogeneous nucleation of Au triggered by concentration fluctuations. The composition of the supercooled droplets may favour the latter process; Si regrowth through a (6 × 6) reconstruction is possible without perturbing this surface structure (Supplementary Fig. 8). This demonstrates that this reconstruction does not inhibit the redeposition of Si at the interface below the droplet while it adapts its composition to follow the Si liquidus line when cooling from above  $T_E$ , reaching the eutectic composition at  $T_E$ . Below  $T_E$ , the droplet's composition is expected to follow the metastable Si liquidus (Fig. 1, step 5). At 513 K, the liquid being Au enriched by ~3–4 at.% with respect to the eutectic composition (Fig. 1), the corresponding degree of supercooling has to be measured between the Au liquidus of the equilibrium phase diagram above  $T_E$  and the metastable (extrapolated) Si

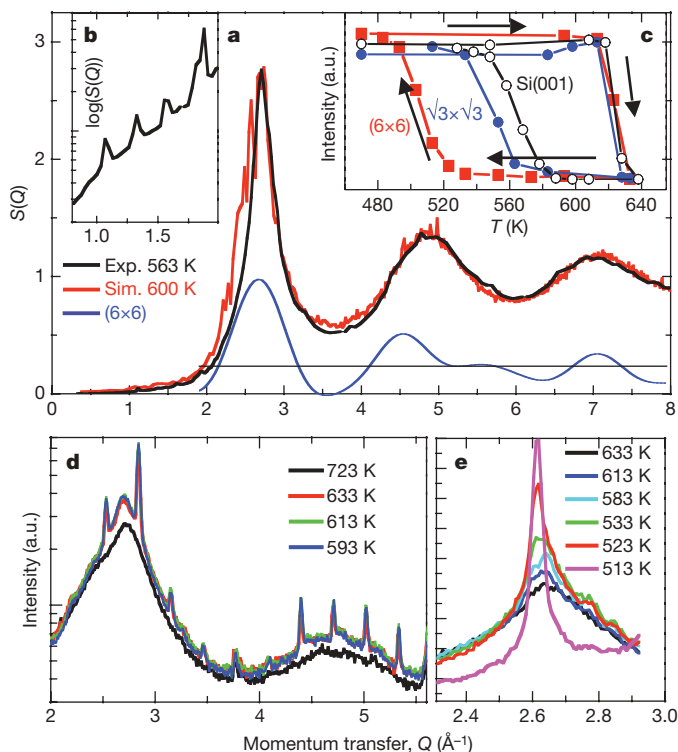


**Figure 3 | Evolution of the liquid structure factor during cooling and solidification.** **a**, Angular average of the experimental structure factor  $S(Q)$  of liquid AuSi at 563 K (black line) together with the theoretical structure factor extracted from MDS at 600 K (red line). The blue line corresponds to the mean structure factor of the  $(6 \times 6)$  reconstruction (Supplementary Fig. 5). **b**, Zoom (logarithmic scale) on the low- $Q$  spectrum of the structure factor, showing the Bragg peaks from two-dimensional crystallites floating on the surface of liquid AuSi (ref. 21). **c**, Hysteresis loops of the integrated intensity of the Au(220) Bragg peak during the solid-liquid-solid transition of Au islands on Si(001) (black open circles), on a Si(111)- $(\sqrt{3} \times \sqrt{3})R30^\circ$  reconstruction (blue filled circles) and on a Si(111)- $(6 \times 6)$  reconstruction (red squares). **d**, Liquid structure factor (logarithmic scale) along the  $\langle 1\bar{1}0 \rangle$  crystallographic direction of the Si(111) surface. The strong influence of the appearance of the  $(6 \times 6)$  reconstruction on the structure of the liquid is visible. **e**, Evolution of the first maximum of the liquid structure factor in the supercooling regime. liquidus below  $T_E$  (red arrow in Fig. 1); this yields a remarkably large value of  $\sim 360$  K.

Our experimental observation is further supported by *ab initio* MDS (see Supplementary Information for details) that allowed monitoring the structural evolution at three temperatures, above and below  $T_E$ . The  $\text{Au}_{81}\text{Si}_{19}$  system was considered to be the prototype liquid for near-eutectic compositions; a change of 3–4 at.% Si does not modify the conclusions drawn from the structural analysis. The alloy was found to stay liquid even at 500 K, that is, well below  $T_E$  (Supplementary Fig. 9). The simulated liquid structure factor  $S(Q)$  compares very well with the experimental one (Fig. 3a), confirming the accuracy of the simulations. To learn more about the detailed three-dimensional picture of the local structure of the liquid, we performed a common-neighbour analysis<sup>24</sup>, which allows us to distinguish between various local structures, such as f.c.c., hexagonal close packed, body centred cubic, and icosahedral environments. The short-range order is found to display an appreciable proportion (46%) of pairs in local five-fold arrangement in the liquid state ( $T = 700$  K); the supercooled regime is characterized by an increased fraction of five-fold atomic ordering (51% at  $T = 600$  K and 54% at  $T = 500$  K). The temperature dependent occurrence of five-fold clusters is shown in Supplementary Fig. 10.

Solid-liquid systems that present important interface-induced atomic layering (that is, short range order like stacking of adjacent liquid layers), such as Al droplets on  $\text{Al}_2\text{O}_3$ , have shown significant supercooling<sup>5,6</sup>, underlining the importance of investigating the

structure, both parallel and perpendicular to the interface, of these interfacial liquid layers. Indeed, the influence of a solid-liquid interface on the five-fold order inside the liquid has been discussed<sup>25,26</sup>. In the present system, we have thus paid particular attention to the structure of the Au-induced  $(6 \times 6)$  reconstruction of the Si(111) surface and its influence on the in-plane structure of the adjacent liquid, revealing a clear link between the structure of this reconstruction and that of the liquid.

Figure 3d shows high resolution measurements of the scattered intensity performed along a symmetry direction of the Si(111) surface, hence crossing its reconstruction peaks. The first and second orders of the liquid structure factor  $S(Q)$  both reveal a marked correlation between the appearance of the  $(6 \times 6)$  reconstruction peaks and an increase in intensity in the maxima of  $S(Q)$ . In addition, the radial intensity distribution obtained by integration of all diffraction peaks measured from the  $(6 \times 6)$  reconstruction and their subsequent convolution by fast Fourier transform (detailed in Supplementary Fig. 6) compares well to the experimental and theoretical structure factors of the liquid (Fig. 3a), indicating close similarities of the main interatomic distances in the liquid and in the  $(6 \times 6)$  structure. Note that our measurements average over a macroscopic surface composed of the free  $(6 \times 6)$  Au reconstructed Si(111) surface between islands, and of the interface between the substrate and the islands; the latter covers only a few per cent of the total area. It is thus not strictly possible to conclude the existence of a long-range ordered  $(6 \times 6)$  reconstruction at the substrate-droplet interface. However, the evidence of enhanced supercooling in the presence of this reconstruction on the one hand, and the high stability of it on the other hand (demonstrated, for example, by its fast recovery by gentle annealing after having been destroyed by ion bombardment) let us believe that the liquid-solid interface is at least locally reconstructed with the pentagonal order of the Au- $(6 \times 6)$  structure.

Zooming in on the first maximum of the liquids'  $S(Q)$  (Fig. 2b) proves that under the influence of the  $(6 \times 6)$  reconstruction, the liquid becomes anisotropic: the scattered intensity is more pronounced in the vicinity of the most intense peaks of the  $(6 \times 6)$  reconstruction, indicating a structural similarity of the  $(6 \times 6)$  structure and the adjacent liquid layers at the local scale. This is further evidenced in Fig. 2c, where scans across the first maximum of  $S(Q)$  are presented for different out of plane momentum transfer,  $Q_z$ . For large  $Q_z$ , the isotropic liquid scattering is separated from a rod of scattering present for all  $Q_z$  at a constant in plane momentum transfer ( $Q_{\parallel}$ ) value. This rod is a signature of a lateral ordering in the liquid close to the solid surface. To interpret this correlation between the internal structure of the liquid and that of the  $(6 \times 6)$  reconstruction, together with the enhanced supercooling, one needs to compare the theoretical and experimental structure of the liquid with the atomic arrangement of the  $(6 \times 6)$  structure.

The detailed atomic structure of the Si(111)- $(6 \times 6)$  Au reconstruction was determined by measuring quantitatively 983 in-plane Bragg superstructure reflections, integrated and corrected for monitor, area, Lorentz and polarization corrections. The in-plane diffraction diagram (Supplementary Fig. 5) has  $p6mm$  symmetry, resulting in 234 non-equivalent reflections with a 4.5% systematic uncertainty. The data were quantitatively analysed using ROD<sup>27</sup> software for surface structure analysis. Scans perpendicular to the surface on several reconstruction rods showed that this  $(6 \times 6)$  superstructure is of monoatomic thickness. The final model ( $\chi^2 = 2.8$  with only the Au atoms taken into account) is remarkably close to the model proposed in ref. 20 for the  $(6 \times 6)$  surface reconstruction induced by a one-monolayer Au deposit. The atomic structure consists of a fairly disordered surface unit of low ( $p31m$ ) symmetry, incoherently scattering with its twin with respect to the  $[1\bar{1}0]$  mirror. It contains several deformed pentagons surrounding the three-fold axes (Fig. 4). The nearest-neighbour distance in these pentagons is 2.86 Å at room temperature, denser than for gold in its bulk f.c.c. structure (2.90 Å at 550 K), but close to the interatomic distance (2.84 Å) in icosahedral Au clusters in the supercooled liquid,

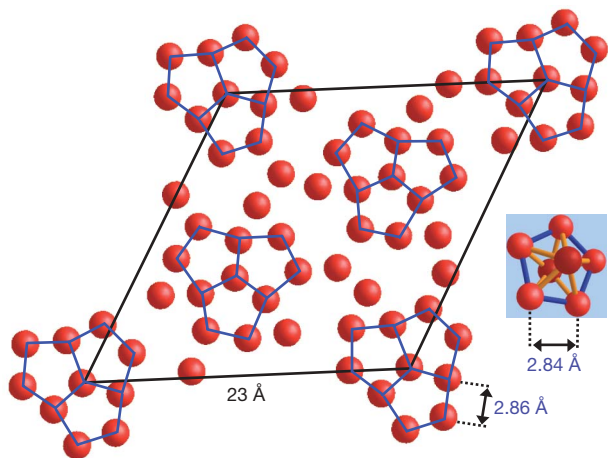


**Figure 4 | Au-induced Si(111)-(6 × 6) surface leading to enhanced supercooling.** Unit cell (black lozenge) of the complex (6 × 6) reconstruction (only the Au atoms are shown) formed at  $T < 673$  K after annealing temperatures  $T > 673$  K. A pentagonal cluster (see inset three-dimensional structure) present in the simulated liquid has similar topology and bond length (2.84 Å) as the surface structure (2.86 Å), smaller than in the Au f.c.c. lattice (2.90 Å). Out of 45 atoms in the unit cell, 30 are in a pentagonal environment (interconnected by blue lines).

as deduced from the MDS (Fig. 4 inset). Thus, the (6 × 6) surface structure offers perfect sites to stabilize the five-fold clusters, which in turn stabilize the supercooled metal.

This much enhanced degree of supercooling of liquid AuSi on the Si(111)-(6 × 6) surface compared to other Si surface structures shows the marked influence of a dense pentagonal atomic arrangement at the solid–liquid interface on the short range order and the metastability of a liquid. Although AuSi can be considered as a liquid with quite unusual properties, pentagonal arrangements have been shown to be favourable in a vast range of liquids<sup>7–11</sup>. More generally, solid–liquid interfaces that favour pentagonal local ordering should lead to deep supercooling, because the origin of the barrier to nucleation of crystallographic phases is the formation of local icosahedral order in the liquid. Such interfaces can significantly affect the liquid in contact with them, thus controlling its stability. This may have important implications—for example, perhaps the containerless techniques required today to obtain supercooling could in the future be replaced by icosahedrally coated solid containers.

## METHODS SUMMARY

**Sample preparation.** After oxide removal, the Si(111) surfaces formed a well-defined Si(111)-(7 × 7) reconstruction. Typically, seven atomic layers of Au were deposited at 300 K (room temperature), forming a 1.6-nm-thick film (Fig. 1, step 1). Owing to the low temperature, the Au film crystalline quality was found to be low, but showed a clear preferential epitaxy with identical directions of the two cubic lattices:  $[1\bar{1}0]\text{Au}(111)||[1\bar{1}0]\text{Si}(111)$ . On heating up to 623 K, which is 13 K below  $T_E = 636$  K (Fig. 1, step 2), the Au film de-wets to form crystalline islands with a preferential in-plane epitaxy rotated by  $19.2^\circ$  with respect to the aligned epitaxy (that is,  $[1\bar{1}0]\text{Au}(111)||[2\bar{3}1]\text{Si}(111)$ ). *In situ* X-ray peak width analysis, together with *ex situ* high resolution secondary electron microscopy and atomic force microscopy, showed islands of average width 150 nm and average height 25 nm (for the seven-monolayer deposit), which is typical for annealed gold layers of similar thickness<sup>28</sup>. Smaller (larger) deposits are expected to lead to smaller (larger) islands. Both Si(111)-(6 × 6) and the  $-(\sqrt{3} \times \sqrt{3})R30^\circ$  reconstructions have been reported on Si(111) for Au coverage around one monolayer. Here the  $(\sqrt{3} \times \sqrt{3})R30^\circ$  is observed whatever the annealing temperature above  $T_E$ . However, it is replaced by the (6 × 6) after annealing above 673 K followed by cooling. More details are available as Supplementary Information.

**Molecular dynamics simulations.** In these simulations, 256 atoms at eutectic composition are arranged in a cubic box with periodic boundary conditions. Canonical NVT (constant number, volume, temperature) ensembles were assumed using the Vienna *ab initio* simulation package<sup>29</sup>. The evolution of the system was followed at three temperatures (700, 600 and 500 K) as a function of

time (durations 30 ps, time step 3 fs), the last two runs being in the supercooled regime. More details are available as Supplementary Information.

Received 13 October 2009; accepted 23 February 2010.

- Turnbull, D. Kinetics of solidification of supercooled liquid mercury droplets. *J. Chem. Phys.* **20**, 411–424 (1952).
- Frank, F. C. Supercooling of liquids. *Proc. R. Soc. Lond. A* **215**, 43–46 (1952).
- Torquato, S. & Jiao, Y. Dense packings of the Platonic and Archimedean solids. *Nature* **460**, 876–879 (2009).
- Reichert, H. *et al.* Observation of five-fold local symmetry in liquid lead. *Nature* **408**, 839–841 (2000).
- Oh, S. H., Kauffmann, Y., Scheu, C., Kaplan, W. D. & Rühle, M. Ordered liquid aluminum at the interface with sapphire. *Science* **310**, 661–663 (2005).
- Greer, A. L. Liquid metals: supercool order. *Nature Mater.* **5**, 13–14 (2006).
- Wochner, P. *et al.* X-ray cross correlation analysis uncovers hidden local symmetries in disordered matter. *Proc. Natl Acad. Sci. USA* **106**, 11511–11514 (2009).
- Steinhardt, P. J., Nelson, D. R. & Ronchetti, M. Icosahedral bond orientational order in supercooled liquids. *Phys. Rev. Lett.* **47**, 1297–1300 (1981).
- Sheng, H. W., Luo, W. K., Alamgir, F. M., Bai, J. M. & Ma, E. Atomic packing and short-to-medium-range order in metallic glasses. *Nature* **439**, 419–425 (2006).
- Schenk, T., Holland-Moritz, D., Simonet, V., Bellissent, R. & Herlach, D. M. Icosahedral short-range order in deeply undercooled metallic melts. *Phys. Rev. Lett.* **89**, 075507 (2002).
- Jakse, N. & Pasturel, A. Local order of liquid and supercooled zirconium by *ab initio* molecular dynamics. *Phys. Rev. Lett.* **91**, 195501 (2003).
- Wagner, R. S. & Ellis, W. C. Vapor-liquid-solid mechanism of single crystal growth. *Appl. Phys. Lett.* **4**, 89–90 (1964).
- Hannon, J. B., Kodambaka, S., Ross, F. M. & Tromp, R. M. The influence of the surface migration of gold on the growth of silicon nanowires. *Nature* **440**, 69–71 (2006).
- Kim, B. J. *et al.* Kinetics of individual nucleation events observed in nanoscale vapor-liquid-solid growth. *Science* **322**, 1070–1073 (2008).
- Kodambaka, S., Tersoff, J., Reuter, M. C. & Ross, F. M. Germanium nanowire growth below the eutectic temperature. *Science* **316**, 729–732 (2007).
- Hofmann, S. *et al.* Ledge-flow-controlled catalyst interface dynamics during Si nanowire growth. *Nature Mater.* **7**, 372–375 (2008).
- Sutter, E. & Sutter, P. Phase diagram of nanoscale alloy particles used for vapor-liquid-solid growth of semiconductor nanowires. *Nano Lett.* **8**, 411–414 (2008).
- Adhikari, H., Marshall, A. F., Chidsey, C. E. D. & McIntyre, P. C. Germanium nanowire epitaxy: shape and orientation control. *Nano Lett.* **6**, 318–323 (2006).
- Pinardi, A. L., Leake, S. J., Felici, R. & Robinson, I. K. Formation of an Au–Si eutectic on a clean silicon surface. *Phys. Rev. B* **79**, 045416 (2009).
- Grozea, D. *et al.* Direct methods determination of the Si(111)-(6 × 6)Au surface structure. *Surf. Sci.* **418**, 32–45 (1998).
- Shpyrko, O. G. *et al.* Surface crystallization in a liquid AuSi alloy. *Science* **313**, 77–80 (2006).
- Chen, H. S. & Turnbull, D. Thermal properties of gold-silicon binary alloy near the eutectic composition. *J. Appl. Phys.* **38**, 3646–3650 (1967).
- Sutter, P. W. & Sutter, E. A. Dispensing and surface-induced crystallization of zeptolitre liquid metal-alloy drops. *Nature Mater.* **6**, 363–366 (2007).
- Honeycutt, J. D. & Andersen, H. C. Molecular-dynamics study of melting and freezing of small Lennard-Jones clusters. *J. Phys. Chem.* **91**, 4950–4963 (1987).
- Spaepen, F. Structural model for solid-liquid interface in monoatomic systems. *Acta Metall.* **23**, 729–743 (1975).
- Heni, M. & Lowen, H. Do liquids exhibit local fivefold symmetry at interfaces? *Phys. Rev. E* **65**, 021501 (2002).
- Vlieg, E. ROD: A program for surface X-ray crystallography. *J. Appl. Crystallogr.* **33**, 401–405 (2000).
- Schubert, L. *et al.* Silicon nanowhiskers grown on 111 > Si substrates by molecular-beam epitaxy. *Appl. Phys. Lett.* **84**, 4968–4970 (2004).
- Kresse, G. & Furthmüller, J. Efficiency of *ab-initio* total energy calculations for metals and semiconductors using a plane-wave basis set. *Comput. Mater. Sci.* **6**, 15–50 (1996).

**Supplementary Information** is linked to the online version of the paper at [www.nature.com/nature](http://www.nature.com/nature).

**Acknowledgements** We thank J. Villain, G. Bauer, H. Reichert, Y. Bréchet and K. Oliver for their reading of the manuscript and T. Duffar, K. Zaidat, P. Guyot and P. Desré for discussions.

**Author Contributions** T.U.S. initiated the work, and contributed to the experimental part; R.D. contributed to both the experimental and theoretical parts; G.R. contributed to the experimental work, A.P. to the theoretical simulations and O.G. to technical assistance. Together with G.R., A.V. analysed the structure of the Si(111)-(6 × 6) reconstruction. T.U.S., G.R., R.D. and A.P. wrote the paper.

**Author Information** Reprints and permissions information is available at [www.nature.com/reprints](http://www.nature.com/reprints). The authors declare no competing financial interests. Correspondence and requests for materials should be addressed to T.U.S. ([schulli@esrf.fr](mailto:schulli@esrf.fr)).